Torque Ripple Reduction Method with Minimized Current RMS Value for SRM Based on Mathematical Model of Magnetization Characteristic

Takahiro Kumagai, Keisuke Kusaka, Jun-ichi Itoh
Nagaoka University of Technology
1603-1 Kamitomioka-cho, Nagaoka city Niigata, Japan
Tel., Fax: +81 / (258) – 47.9533.
E-Mail: kumagai_t1125@stn.nagaokaut.ac.jp, kusaka@vos.nagaokaut.ac.jp,
itoh@vos.nagaokaut.ac.jp
URL: http://itohserver01.nagaokaut.ac.jp/itohlab/index.html

Keywords

«Switched reluctance drive», «Electrical drive», «Ohmic Losses»

Abstract

This paper proposes a torque ripple reduction method with minimum current RMS value for switched reluctance motors (SRM). In the proposed method, the current waveform to achieve constant torque is derived based on a mathematical model of magnetization characteristics. In particular, the current waveform is optimized in term of the reduction of the current RMS value and the satisfaction of the input voltage limitation. The algorithm for determining the torque command is introduced to derive current command which is possible to generate by the input voltage and lead to the design of the maximum torque per current RMS value without any complex and time-consuming computation process. A three-phase 18S/12P type SRM is used in simulation and experiment in order to validate the proposed method. As a result, the reduction of torque ripple by 65.8% and the reduction of the current RMS value by 19.2% are achieved by proposed method.

I. Introduction

In the last decade, researches on switched reluctance motor (SRM) have been accelerated due to an increasing demand of electric vehicle. SRM consists of only an iron core and concentrated windings, which can achieve rare-earth-element-free and low manufacturing cost. In addition, the rotor is built with a solid salient pole core structure, which is suitable for high speed rotation with low inertia. In SRM, one-phase excitation mode is applied as a general control method [1][2]. In this method, the continuous rotation of the motor is achieved by the excitation of each phase stator winding at an appropriate timing. However, a large torque ripple still occurs in the torque since the torque decreases during the switching phase interval. In order to overcome this problem in SRM, many control methods have been studied actively with the development of the power electronics technology in recent years [3]-[10].

The control method is proposed in order to reduce the torque ripple by the excitation of two phase stator windings during the switching phase interval [3]-[10]. In this method, several current waveforms which obtains an instantaneous torque without any ripple, i.e. the constant torque, is obtained from the magnetization characteristic. In this paper, the current waveform which obtains the constant torque is referred to as the constant-torque current waveform.

However, in the conventional method, the current root-mean-square (RMS) value significantly increases due to the high current peak occurring in the motor current during the switching phase interval [10]. This is because the conventional method chooses the constant-torque current waveform which is not optimized in order to both eliminate the torque ripple and reduce the current RMS value. In particular, the switching phase interval starts when the generable torque from one phase has already become very small. As a result, the current from the other phase has to be large in order to generate sufficient torque and maintain the constant torque. In order to reduce the current peak, the starting point is designed so that the generable torque from one phase is still large. Nevertheless, in this case, the required slope of the current from the other phase might not be sufficient due to the limitation of the input voltage. If the constant-torque current waveform which is impossible to generate by the input voltage is applied, torque ripple still occurs in the torque.

In SRM, it is not clear how to properly obtain the constant-torque current waveform which satisfies both the voltage limitation and the current reduction of the inverter due to the nonlinear magnetization characteristic of SRM. In order to achieve the above objectives, the constant-torque current waveform is optimized by considering both current reduction and voltage limitation of the inverter. In general, first, several constant-torque current waveforms are derived by the variation of the parameters value determining the shape of the waveform; next, the optimized current waveform is selected [7]-[9]. However, the common disadvantage of these conventional methods is that the derivation of the constant-torque is time-consuming and has to be conducted whenever the motor is changed.

This paper proposes a torque ripple reduction method considering the current RMS value and the input voltage limitation. The constant-torque current waveforms are derived by the mathematical model of the magnetization characteristic, which reduces the computation time [10]. In addition, the constant-torque current waveform is optimized in term of the reduction of the current RMS value and the satisfaction of the input voltage limitation. This leads to the design of the maximum torque per current RMS value without any complex and time-consuming computation process.

This paper is organized as follows; first the derivation method of the constant-torque current waveforms based on the mathematical model of the magnetization characteristic is explained. Next, the algorithm for the determination of the ideal constant-torque current waveform which is possible to achieve simultaneously the torque ripple reduction and the current RMS value reduction. Finally, the simulation and experimental results are shown in order to confirm the validity of the proposed method.

II. TORQUE GENARATION MECHANISM IN SRM

In SRM, the torque T is generated by the change of magnetic co-energy W_c depending on the saliency between the stator and rotor which is caused by the change of the rotor position θ_m, [1][11]

$$T(i,\theta_m)=\frac{\partial W_C(i,\theta_m)}{\partial\theta_m}=\frac{\partial}{\partial\theta_m}\int_0^i\Phi(i',\theta_m)di' \tag{1}$$

where Φ is the flux linkage, i is the current, and i' is the integral variable defined on the interval [0, i]. Note that W_c equals to the surface areas surrounded by the magnetization curve and the current axis in the magnetization characteristic. In order to obtain the instantaneous torque, the flux linkage Φ in (1) is mathematically derived based on the method which has already been proposed in [10].

Table I shows the motor parameters of the evaluated SRM. A three-phase 18S/12P type SRM is chosen as an example to investigate.

Fig. 1 depicts the magnetization characteristic of the evaluated SRM. The flux linkage Φ is a function of the position (electrical angle) θ_e and the current i. The flux linkage Φ changes periodically between the aligned flux linkage Φ_a and the unaligned flux linkage Φ_u, and expressed as in (2), [10]

$$\Phi(i,\theta_m)=\Phi_u(i)+f(\theta_e)(\Phi_a(i)-\Phi_u(i)) \tag{2}$$

The periodic function $f(\theta_e)$ is approximated by the fundamental harmonic and the second-to-tenth-order harmonics of the cosine function as shown in (3),

$$f(\theta_e)=\frac{1+\cos(\theta_e)+\sum_{n=2}^{10}h_n((-1)^{n-1}+\cos(n\theta_e))}{2(1+h_3+h_5+h_7+h_9)} \tag{3}$$

where h_n is the content rate of the n-order harmonic component. Next, the rotation electrical angle θ_e is considered in the range of -π to 0, where θ_e=0 indicates the alignment state, and θ_e =-π indicates the complete unalignment state. Substituting (2) into (1), the torque is expressed as in (4).

$$T(i,\theta_m)=\frac{\partial f(\theta_e)}{\partial\theta_m}\int_0^i(\Phi_a(i)-\Phi_u(i))di' \tag{4}$$

In the linear region, the aligned flux linkage $\Phi_a(i)$ and the unaligned flux linkage $\Phi_u(i)$ are expressed as in (5),

$$\begin{cases}\Phi_u(i)=L_u i\\ \Phi_a(i)=L_a i\end{cases} \tag{5}$$

where L_a is the initial aligned stator inductance and L_u is the unaligned stator inductance. Substituting (5) into (4), the torque in the linear region is expressed as in (6).

$$T(i,\theta_m) = \frac{\partial f(\theta_e)}{\partial \theta} \frac{(L_a - L_u)i^2}{2} \tag{6}$$

In the saturation region, the aligned flux linkage $\Phi_a(i)$ and the unaligned flux linkage $\Phi_u(i)$ are expressed as in (7),

$$\begin{cases} \Phi_u(i) = L_u i \\ \Phi_a(i) = \Phi_{sat}\left\{1-(1+Ki)e^{-\tau i}\right\} + L_{sat} i \end{cases} \tag{7}$$

where L_{sat} is the saturated aligned stator inductance, Φ_{sat} is the aligned saturation flux linkage, and τ is the coefficient which is determined to minimize the sum of the squares of the residuals between the magnetic characteristic and (7) in the alignment state. In order to maintain the continuity of the inductance in the low current range and (3), K is expressed as in (8),

$$K = \tau - \frac{L_a - L_{sat}}{\Phi_{sat}} \tag{8}$$

Substituting (7) into (4), the torque in the saturated region is expressed as in (9).

$$T(i,\theta_m) = \frac{\partial f(\theta_e)}{\partial \theta_m}\left\{\Phi_{sat}\left(i + \frac{K+\tau+K\tau i}{\tau^2} e^{-\tau i}\right) + \frac{L_{sat} - L_U}{2} i^2 + T_o\right\} \tag{9}$$

Let the current value of the boundary of the linear region and the saturation region be I_0 , the value of the torque at the boundary T_0 is expressed as in (10),

$$T_o = \frac{L_a - L_{sat}}{2} I_o^2 - \Phi_{sat}\left(I_o + \frac{K+\tau+K\tau I_o}{\tau^2} e^{-\tau I_o}\right) \tag{10}$$

Fig. 2 depicts the T-i-θ_m characteristic obtained by calculating the formula $T(i,\theta_m)$ at the values of the current from 20A to 300A and the rotor position. It is observed from Fig. 2 that a required current value for any torque at any rotor position is calculated.

TABLE I. MOTOR PARAMETERS OF SRM.

Rated mechanical power P_m	5.5 kW
Rated speed ω_n	12000 r/min
Rated torque T_n	9.3 Nm
Input voltage	48V
Number of poles	Rotor 12, Stator 18
Winding resistance R	0.011 Ω
Number of coil turns	12 turns

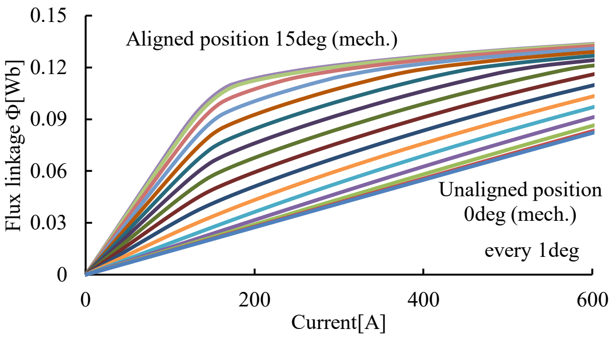

Fig. 1. Magnetization characteristic.

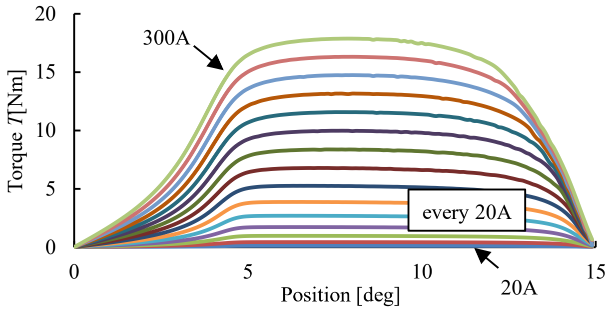

Fig. 2. T-i-θ_m characteristic.

A. Torque sharing function

In this subsection, the control method of each phase torque, which removes the torque ripple from the motor shaft torque is explained. In this paper, the torque sharing function $f_{Tx}(\theta_m)$ [3] which represents the sharing rate of each phase torque according to the rotor position, is introduced to derive the constant-torque current waveforms. Generally, the application of the torque sharing function $f_{Tx}(\theta_m)$ is proposed in the conventional derivation method [6]-[10].

Fig. 3 shows the example of the torque sharing function $f_{Tx}(\theta_m)$. The sum of each phase torque is the constant torque. Note that the subscript x indicates the phase in the torque sharing function $f_{Tx}(\theta_m)$. Each individual phase generates the torque during the one-phase conduction period, whereas two phases generate the torque during the two-phase conduction period, i.e. the switching phase interval. In order to make the sum of each phase torque result in the torque with no ripple, i.e. a constant torque, f_{Tx} becomes 1 during one-phase conduction period, whereas the sum of two-phase f_{Tx} equals to 1 during two-phase conduction period (the period θ_{lap} in the figure). It is observed that various functions is selected for the torque sharing function. In this paper, the cosine function is utilized in order to avoid a steep rise [4]. Therefore, the torque sharing function is expressed as in (11),

$$f_{Tx}(\theta_m) = \begin{cases} \dfrac{1}{2}\left\{\cos(\dfrac{\theta_m - \theta_{f0}}{\theta_{lap}})\pi + 1\right\} & \theta_0 \le \theta_m \le \theta_{f0} \\ 1 & \theta_{f0} \le \theta_m \le \theta_{fc} \\ \dfrac{1}{2}\left\{\cos(\dfrac{\theta_m - \theta_{fc}}{\theta_{lap}})\pi + 1\right\} & \theta_{fc} \le \theta_m \le \theta_c \\ 0 & otherwise \end{cases} \tag{11}$$

where θ_{lap} represents the length of the two-phase conduction period, and θ_{f0} indicates the initial angle of the next one-phase conduction period, i.e. the end point of the two-phase conduction period. In the SRM with number of phases m, number of stator pole N_s, and number of rotor poles N_r structure, since the conduction period of the adjacent phase shifts the angle of $2\pi/mN_r$ rad in the mechanical angle, the turn-on angle θ_0, the ending angle θ_{fc} of the one-phase conduction period, and the turn-off angle θ_c are expressed by (12) as dependent variables of θ_{lap} and θ_{f0},

$$\theta_0 = \theta_{f0} - \theta_{lap}, \theta_{fc} = \theta_0 + \frac{2\pi}{mN_r}, \theta_c = \theta_{f0} + \frac{2\pi}{mN_r} \tag{12}$$

Therefore, the torque sharing function $f_{Tx}(\theta_m)$ can be determined as the independent variable of θ_{lap} and θ_{f0}. The torque of each phase is controlled accurately by the multiplication of (11) with the torque command T^*, eliminating completely the torque ripple. Consequently, the following (13) should be satisfied.

$$T(i^*, \theta_m) = T^* f_{Tx}(\theta_m) \tag{13}$$

The instantaneous command current value is calculated from (13). If the current follows exactly the command current, the torque becomes theoretically constant.

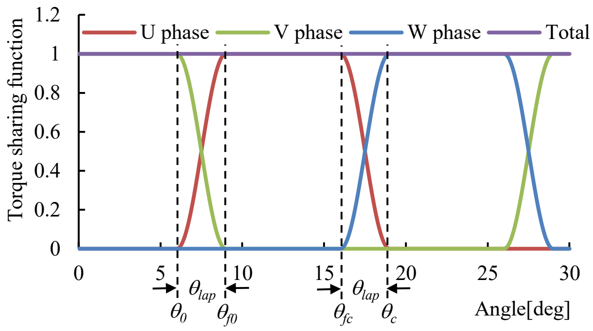

Fig. 3. Torque sharing function which represents the sharing rate of each phase torque according to the rotor position.

III. DERIVATION OF IDEAL CURRENT WAVEFORM

A. Consideration of Input Voltage Limitation

The torque ripple still occurs in the torque if the constant-torque current waveform which is impossible to generate by the input voltage is employed. In this subsection, in order to derive the constant-torque current waveform considering the input voltage limitation, the derivation method of the variables θ_{f0} and θ_{lap}, which determine the two-phase conduction period, is explained [10].

The margin M is defined as the difference between the maximum current slope, which is possible to generate by the input voltage, and the constant-torque current slope. The constant-torque current waveform is applicable when the margin M is positive. Otherwise, the torque is not achieved with the selected constant-torque waveform. The angle where the margin M becomes the minimum is either the initial angle of the one-phase conduction period or the turn-off angle. Therefore, first, M is derived at these two angles. Next, it is determined that the variables θ_{f0} and θ_{lap} which satisfies $M \geqq 0$ at these two angles.

The margin M_f is expressed as in (14) when the current rises,

$$M_f = \frac{E_d}{L_u + f(\theta_{f0} - \theta_{lap})(L_a - L_u)} - \frac{\omega\pi}{\theta_{lap}}\sqrt{\frac{T^*}{2(L_a - L_u)}}\left(\frac{df(\theta_{f0} - \theta_{lap})}{d\theta_m}\right)^{-1/2} \tag{14}$$

On the other hand, the margin M_l is given by (15) when the current falls,

$$M_l = \frac{E_d}{L_u + f(\frac{2\pi}{mN_r} + \theta_{f0})(L_a - L_u)} - \frac{\omega\pi}{\theta_{lap}}\sqrt{\frac{T^*}{2(L_a - L_u)}}\left(\frac{df(\frac{2\pi}{mN_r} + \theta_{f0})}{d\theta_m}\right)^{-1/2} \tag{15}$$

where E_d is input voltage. In order to derive the constant-torque current waveform that satisfies the input voltage limitation, θ_{lap} is determined under the condition that $M_f \leqq 0$ by the adjustment of θ_{f0} at M_l=0.

B. Consideration of Current Limitation

In this subsection, the design of the variables θ_{f0} and θ_{lap}, resulting in the constant-torque current waveform with minimum current RMS value, is explained.

Fig. 4 depicts the flowchart for the derivation of the ideal constant-torque current waveform. In order to achieve the constant torque with minimum current RMS value during the two-phase conduction period, it is necessary to generate the torque during the interval where the generable torque is still high under the condition that $M \geqq 0$ is satisfied. First, the ideal two-phase conduction period, which is achieves the maximum torque per current value, is calculated under the condition that the input voltage is limitless, i.e. neglecting the limitation of the input voltage. Next, the actual two-phase conduction period satisfying $M \geqq 0$, i.e. the consideration of the input voltage limitation, is designed as

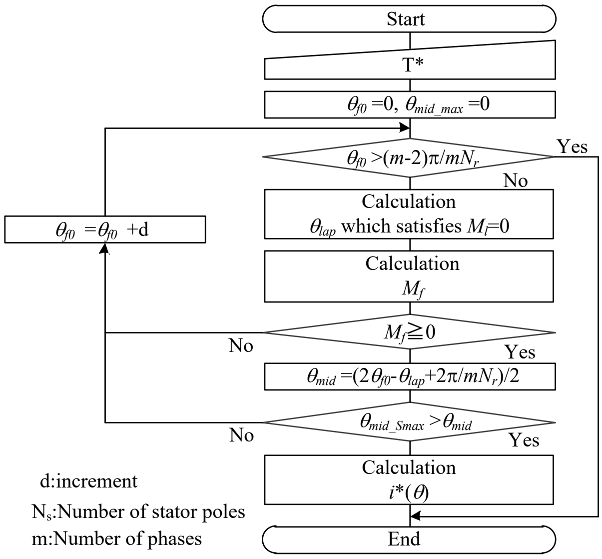

Fig. 4. Generation flow for ideal current waveform which is possible to generate by the input voltage and lead to the design of the maximum torque per current RMS value.

close as possible to the calculated ideal two-phase conduction period. In particular, the calculation of the ideal two-phase conduction period is explained as follows.

Fig. 5 shows the relationship between the variables θ_{f0} and the magnetic co-energy W neglecting the input voltage limitation. The magnetic co-energy W is the integral of the average torque over one cycle (2π). Therefore, the maximum torque per current value is achieved when the magnetic co-energy W becomes the largest. Meanwhile, the magnetic co-energy W in one cycle of current path equals to the surface area enclosed by the current path as shown in Fig. 2. Hence, the magnetic co-energy W during the conduction period [θ_{f0}, $\theta_{f0}+2\pi/mN_r$] is expressed in (10),

$$W = (f(\theta_{f0} + 2\pi/mN_r) - f(\theta_{f0}))\int_0^I (\Phi_a(i) - \Phi_u(i))di \tag{16}$$

Note that the term of the integral in (10) indicates the magnetic co-energy W_o between the alignment state and the unalignment state. This magnetic co-energy W_o is constant and depends only on motor parameters. Therefore, the magnetic energy W becomes the largest by the maximization of $f(\theta_{f0}+ 2\pi/mN_r)$-$f(\theta_{f0})$. As shown in Fig. 5, the maximum magnetic energy W is achieved at θ_{f0_Wmax} of 3.98 deg.. Then, the middle angle of the conduction period θ_{mid_Wmax} which can maximize W is expressed as in (11).

$$\theta_{mid\_W\max} = \theta_{f0\_\max} + \pi/mN_r \tag{17}$$

On the other hand, the middle angle of conduction period θ_{mid} as shown in Fig. 3 is expressed as in (12).

$$\theta_{mid} = \frac{2\theta_{f0} - \theta_{lap} + 2\pi/mN_r}{2} \tag{18}$$

Under the condition of the limitless input voltage, the selection of θ_{f0_Wmax} of 3.98 deg. results in θ_{mid_Wmax} of 8.98 deg.. Therefore, when considering the input voltage limitation, the actual θ_{f0} should be selected such that the actual θ_{mid} becomes as close as possible to θ_{mid_Wmax}.

IV. SIMULATION AND EXPERIMENTAL RESULTS

A. Validation of proposed algorithm

A three-phase 18S/12P type SRM is used in order to validate the proposed method. The hysteresis comparator is employed as the current control. In the simulation, the maximum hysteresis error is designed to be small enough to evaluate the torque ripple caused only by the follow or non-follow of the current to the ideal current waveform.

Fig. 6 shows the relationship between θ_{f0} and M_f when varying the value of θ_{f0} during the former half of the conduction period, i.e. the period when the current rises. Note that the input voltage limitation is considered. At each value of θ_{f0}, first, θ_{lap} is derived by (9) when M_l=0; then the margin M_f is calculated by substituting the values of θ_{f0} and θ_{lap} into (8). As shown in Fig. 6, the region where $M_f \geqq 0$ represents the values of θ_{f0}, the applicable region of the constant-torque current waveform. On the other hand, the region where $M_f<0$ represents the values of θ_{f0} where there is no applicable constant-torque current waveform.

Fig. 7 shows the relationship between θ_{f0} and θ_{mid} when varying the value of θ_{f0}. If θ_{f0} of 4.65 deg. is selected, θ_{mid} becomes the closet value to θ_{mid_Wmax}. Hence, this selection of θ_{f0} leads to the constant-torque current waveform with the minimum current RMS current value applicable with the given input voltage.

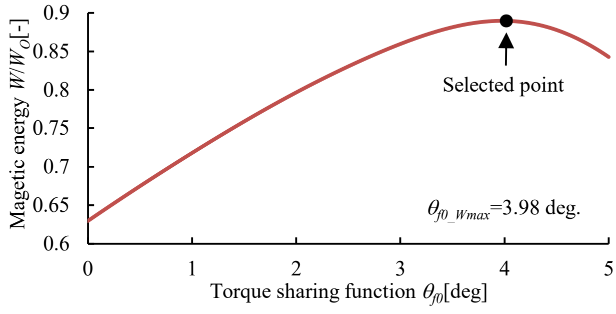

Fig. 5. Calculated magnetic co-energy $W/Wo = f(\theta_{f0}+ 2\pi/mN_r)$-$f(\theta_{f0})$

Fig. 8 shows the relationship between rotation speed and the middle angle of the conduction period θ_{mid}. The graph is divided by a dashed line at θ_{mid_Wmax} of 8.98 deg.. The constant-torque current waveforms under this dashed line are applicable at low rotation speed, which means that θ_{mid} should be chosen as close as possible to this dashed line in order to minimize the current RMS value. However, at high rotation speed, the applicable θ_{mid} becomes lower because the current slope during the two-phase conduction period is limited by the input voltage as shown in point (a). In the conventional method, the same θ_{mid} is chosen over entire rotation speed as point (b) shown in Fig. 8, whereas in the proposed method, θ_{mid} is chosen to be as close as possible to θ_{mid_Wmax} at every single rotation speed as points (c) in Fig. 8. Therefore, the current RMS value can be reduced at low rotation speed with the proposed method.

Fig. 9 shows the current paths in the magnetization characteristic for each designed points (a), (b), and, (c) of Fig. 8. The ideal current path with the minimum current RMS value is shown as a dashed line. The current path with the designed points (a) and (b) of Fig. 8 do not follow the ideal current path, leading to the increase in the current peak. On the other hand, the designed point (c) of Fig. 8 follows the ideal current path, resulting in the minimum current peak.

Fig. 10 shows the waveforms of the current, and the torque at three designed points (a), (b) and (c) of Fig. 8. As shown in Fig.10, in all cases, an instantaneous torque without any ripple, i.e. the constant torque, is achieved. Comparing Fig. 10(b) and (c), the proposed method suppresses the high current

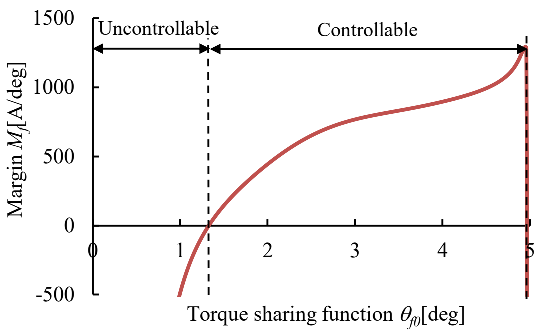

Fig. 6. Margin of the current slop in former half of conduction period.

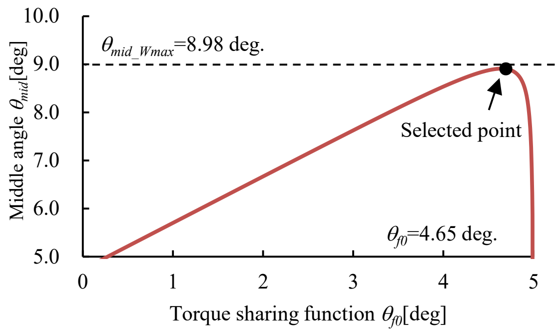

Fig. 7. Calculated value of the middle angle when varying the value of torque sharing function

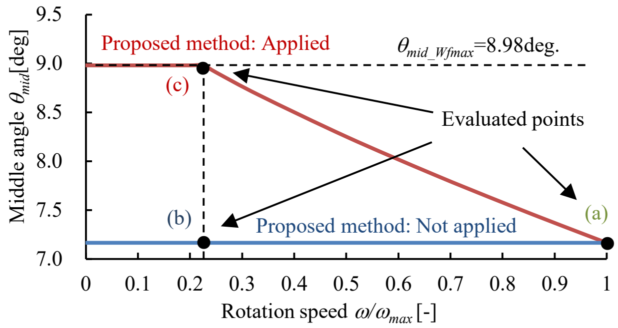

Fig. 8. Relationship between rotation speed and middle angle θ_{mid}, the rotation speed 1 p.u. is defined as the maximum rotation speed under no torque ripple at rated torque, i.e. M_f and M_l are 0, and further optimization is impossible.(T_n=4.91Nm, V_n=48V, ω_{max}=98.3[rad/s])

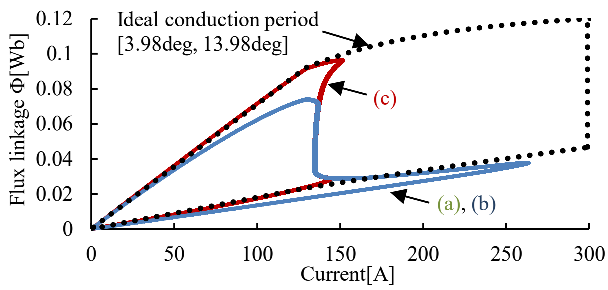

Fig. 9. Current paths in magnetization characteristic

peak occurring during the switching interval at low rotation speed, leading to the reduction of the current RMS current value.

Fig. 11 shows the relationship between the rotation speed and the current RMS value with the conventional and proposed method. As shown in Fig. 11, comparing the conventional method, the current RMS value reduction with the proposed method becomes more effective at low rotation speed. In particular, the current RMS value is reduced by 21.2% at most. Thus, the effectiveness of the proposed method is confirmed by these results.

Fig. 12 shows the relationship between the rotation speed and the current peak value with the conventional and proposed method. As shown in Fig.12, the current peak value is reduced, and the maximum reduction is 43.2%. Note that there is a trade-off between the RMS value and peak value of current. Therefore, it is not concluded that these peak values are the minimum values. However, the peak value is reduced in all range. Thus, the effectiveness of the proposed method is confirmed by these results.

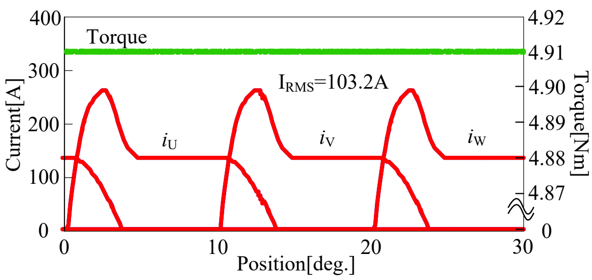

(a) Rotation speed: 1 p.u.

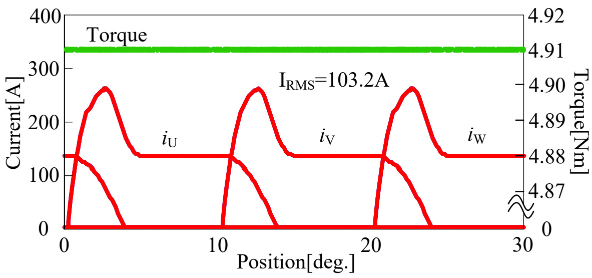

(b) Rotation speed: 0.25 p.u. Conventional method

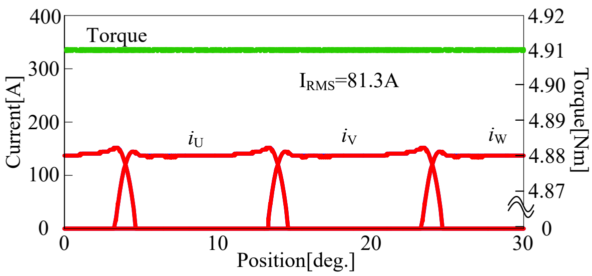

(c) Rotation speed: 0.25 p.u. Proposed method

Fig. 10 Current waveform and Output torque.

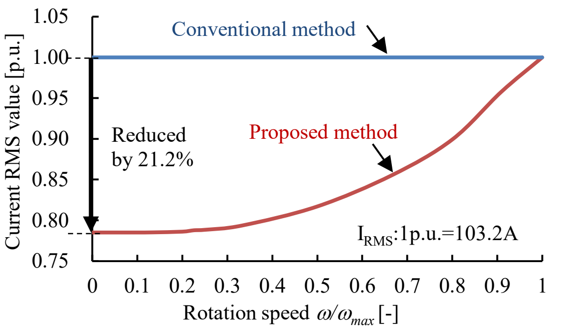

Fig. 11 Relationship between rotation speed and current peak value

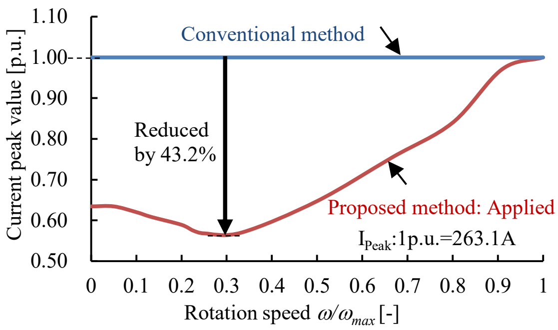

Fig. 12 Relationship between rotation speed and current peak value

B. Experimental Results of ideal current waveform

The effectiveness of the proposed method is confirmed by experiment. In order to realize high-speed current control and reduce the torque ripple caused by the hysteresis error, current-hysteresis controller is constructed by analog circuit. In the experiment, the maximum hysteresis error designed to be 10A regulated by the switching of the switching devices. In addition, in order to evaluate the torque ripple excluding the component caused by the hysteresis error, the low-pass filter (LPF) with a cutoff frequency of 1.6kHz is applied to the torque signal.

Fig. 13 shows the current waveforms, the torque waveforms, and the harmonic components of the torque with one-phase excitation mode, the conventional and proposed ripple torque reduction method based on two-phase excitation mode. Large torque ripple occurs in SRM during switching phase interval. Therefore, the fundamental frequency of the torque ripple is $3NrN/60=207$Hz in the experimental condition The torque ripples of the two-phase excitation mode as shown Fig. 13 (b) and (c) are reduced by 67.0% and 65.8 % compared with the one-phase excitation mode in Fig. 13 (a), respectively. In addition, the fundamental component of the torque ripple is reduced by 88.6% and 93.2% respectively. Furthermore, the current RMS value of the proposed torque reduction method in Fig. 13 (c) is reduced by 19.2% compared with that of the conventional torque reduction method in Fig. 13 (b). Furthermore, the current peak value is reduced by 32.1%. Therefore, the ideal current

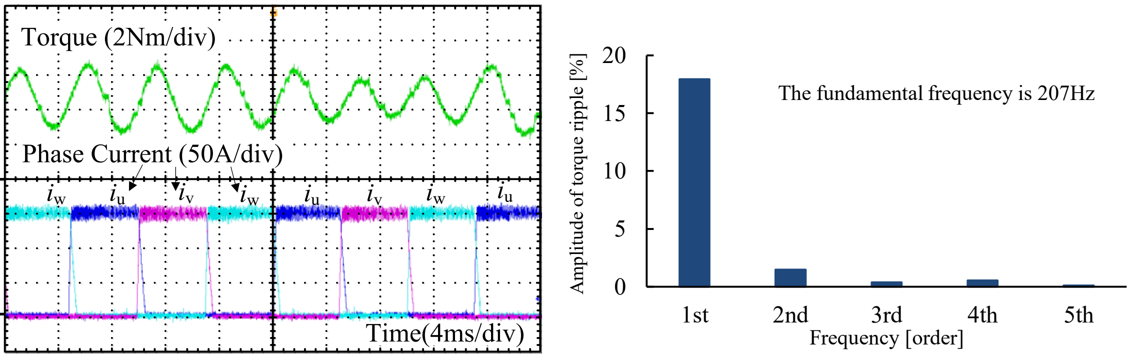

(a) One-phase excitation mode (I_{RMS}=80.8A, I_{peak}=140A, Torque ripple=77.9%)

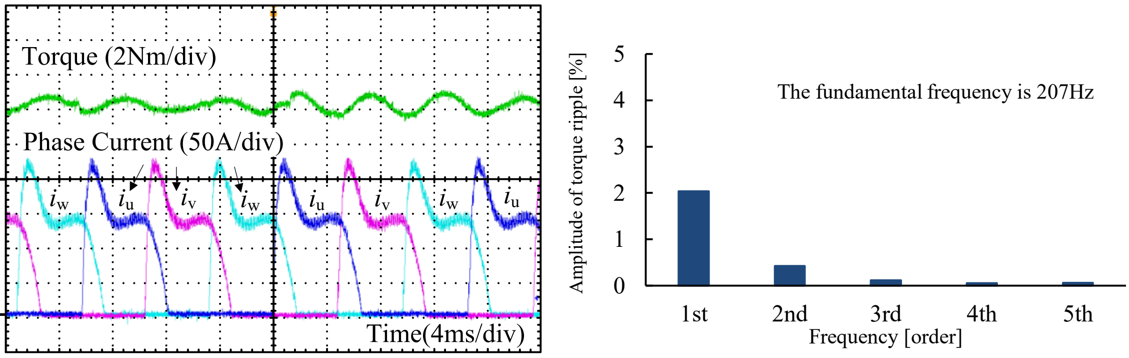

(b) Conventional method (Command: I_{RMS}=94.8A, I_{peak}=215.4A, Torque ripple=25.7%)

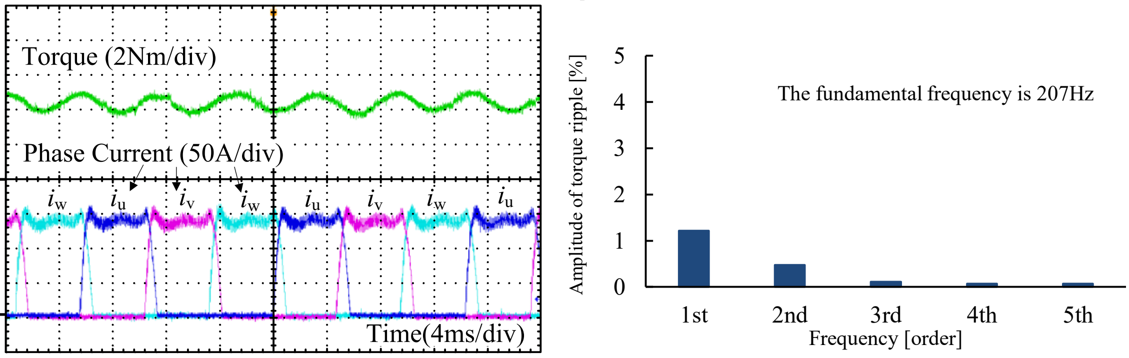

(c) Proposed method (Command: I_{RMS}=79.5A, I_{peak}=146.1A, Torque ripple=26.6%)

Fig. 13 The current waveforms, the torque waveforms, and the harmonic components of the torque at T^*=4.91Nm, Rotation speed: 345rpm.

waveform to achieve the constant torque with the minimized current RMS value is confirmed. Note that the torque ripple still occurs even if the constant-torque current waveform is applied. This is because the torque ripple is caused by model inaccuracies of magnetization characteristic.

V. Conclusion

This paper proposed the torque ripple reduction method considering the input voltage limitation and the minimization of the current RMS. In the proposed method, the design algorithm was employed to determine the ideal constant-torque current waveform which was possible to achieve simultaneously constant torque and the current RMS value reduction. It was confirmed from the simulation and experiment results that the reduction of torque ripple by 65.8% and the reduction of the current RMS value by 19.2% are achieved by proposed method. In other words, the copper loss is reduced by 34.7% by proposed method.

References

[1] T. J. E. Miller:"Switched Reluctance Motors and their Control", MAGNA PHYSICS PUBLISHING OXFORD SCIENCE PUBLICATION (1993).

[2] Y. Ishihara, M. Sugiura, H. Ishikawa, H. Naitoh:" Improving the Efficiency of Switched Reluctance Motors using a Step-Skewed Rotor", IEEJ Journal of Industry Application, Vol.4 No.4 pp.445-453 (2015)

[3] I. Husain, M. Ehsani: "Torque Ripple Minimization in Switched Reluctance Motor Drives by PWM Current Control", IEEE Trans., vol.11, no.1 (1996)

[4] K. Russa, I. Husain, M. Elbuluk, "Torque-Ripple minimization of switched reluctance machines over a wide speed range", IEEE Trans. On Industry Applications, vol. 34, no. 5, pp. 1105-1112, 1998.

[5] Khwaja M. Rahman, Steven E. Schulz: "High-Performance Fully Digital Switched Reluctance Motor Controller for Vehicle Propulsion", IEEE Trans. on Industry Applications, vol.38, no.4, pp1062-1071(2002).

[6] H X. D. Xue, K. W. E. Cheng, S. L. Ho, "Optimization and evaluation of torque-sharing functions for torque ripple minimization in switched reluctance motor drives," IEEE Trans. Power Electronics, vol. 24, no. 9, pp. 2076-2090, Sep. 2009.

[7] J.W. Ahn, "Torque control strategy for high performance SR drives", Journal of Electrical Engineering & Technology, vol. 3, no. 4, pp 538-545, 2008.

[8] Milad Dowlatshahi, Seyed M. Saghaiannejad, Jin-Woo Ahn, and Mehdi Moallem, "Minimization of Torque-Ripple in Switched Reluctance Motors Over Wide Speed Range" J Electr Eng Technol Vol. 9, No. 2: 478-488, 2014

[9] H. ISHIKAWA, Y. KAWADA, and H NAITOH, "Instantaneous Current Profile Control for Flat torque of Switched Reluctance Motors", Electrical Engineering in Japan, Vol. 163, No.3, 2008.

[10] T. Kumagai, D. Sato, and J. Itoh, "Torque Ripple Reduction Method for SRM based on Mathematical Model considering Voltage Limitation", EPE2017, Vol. DS1g, No. 0392 (2017).

[11] Senad Smaka :" Fast Analytical Model for Switched Reluctance Machines", IEEJ Journal of Industry Application, Vol.4 No.4 pp.352-359 (2015)